

## CHAPTER 10

# Computer-aided engineering findings on the physics of tire/road noise

**Laith Egab**

School of Engineering, RMIT University, Melbourne, VIC, Australia

### 10.1 Introduction

The simulation of the tire/road noise has gained remarkable attention in recent years. This is because of the increasing demand for the vehicle performance and intense competition among tire manufacturers. Tires are made from many different components from the softest solid materials to tough and hard materials like textile fibers and steels, which are one of the most complex composites.

The prediction of tire performance from simulations is a challenge, not only due to the materials the tires are made from, but also because of the presence of a highly nonlinear structure in the tires, as well as dynamic contact boundary conditions. In order to reduce the product development time, computer-aided engineering (CAE) and simulation tools are already popular for use in tire industries. The simulation of vehicles and their tires has become one of the very important aspects of the tire design and failure analysis for most of tire companies. Simulation technology or capability has been developed in almost all important areas such as the performance prediction, design, optimization, and manufacturing. This means in the areas such as structure design, manufacturing, performance prediction, and optimization. New CAE simulation tools have enabled investigation of the tire/road noise in the early stages of the design process by performing most of the analyses using virtual models. Also, the application of other optimization techniques such as the Genetic Algorithm (GA) technique can help in performing sensitivity analysis and optimization studies by postprocessing the CAE analysis results.

The complexity of the tire models has evolved throughout time. New modeling techniques and more powerful computational tools are continuously being developed and introduced. The simpler models of the tire structure are presented using a lumped parameter approach that discretizes the tire belt into an elastic ring, string, or beam suspended on an elastic/plastic foundation. These models require tests to identify the equivalent lumped properties of the system. This procedure is highly dependent on the discretization level of the system in addition to the type of the forced elements that are used between the system components. Additionally, these models, due to their simplified approach, lack some of the system informative factors, such as precise local defamations of the contact patch and complete response spectrum of the system (e.g., frequency content of the response).

The more detailed are considered in the tire models that incorporate finite element methodology to discretize the tire structure to a higher extent, resulting in more complex models. For parameterizing the FEM tire models, experimental tests need to be conducted to fully define the material properties to be used in the code. Once the material properties are fully defined, the FEM tire models can be used in various design contexts without the need to characterize the system again, similar to the lumped parameter approaches. All of these activities come at the cost of more tedious modeling efforts and longer computational time. In addition to the aforementioned models, there are also some semianalytical semifinite element models that consider a simplification of the actual problem in order to incorporate the tire experimental data in a way so that the tire mechanics can be fully illustrated with less computational effort.

In this chapter, the methodologies, challenges, and perspectives of developing a tire model for the vehicle simulation are discussed. First the CAE methodologies like the finite element method (FEM), the boundary element method (BEM), the waveguide finite element method (WFEM), as well as statistical energy analysis (SEA), energy finite element analysis (EFEA), computational fluid dynamics (CFD), and transfer path analysis (TPA) are presented and discussed. Vehicle suspension corner module is discussed and the mechanisms of the wheel imbalance, wheel force variation, and wheel impact force related friction are described and analyzed. Then the auralization models of tire/road noise and the current trends and challenges in the CAE modeling of tire/road noise are included. Finally, the chapter will conclude with a summary.

## 10.2 Computer-aided engineering simulation methodologies

This section covers state-of-the-art methodologies in tire/road noise modeling and simulations and outlines different classes of CAE methodologies. Deterministic methods are applied in the low frequencies, energy methods are applied in the high frequencies, and hybrid methods are applied in the mid frequencies.

### 10.2.1 Deterministic methods at low frequency

In the low frequency range, the characteristic length of the system is smaller than or in the same order of magnitude as the dominant physical wavelengths of the dynamic response. The response of the system is determined by well-separated modes and can be predicted by means of deterministic numerical methods. In particular, the FEM and BEM are most commonly applied in the low frequency range.

#### 10.2.1.1 Finite element method

The mechanical behavior of the tire depends on many parameters, such as tire geometrical and material property parameters. Identifying these parameters and correlating them to the vehicle performance using empirical models might have limitation due to similar test conditions. On the other hand, using simple physical models for estimating the vehicle performance from the model input parameters might lead to significant errors. One alternative numerical method for analyzing tire dynamics is the FEM. The FEM is an efficient and low-cost numerical method that can be used for complicated tire dynamic analysis. The method represents the geometry of each single component by a set of numerous small sized elements (finite elements). Within these elements, field variables such as structural displacement and acoustic pressure are described in terms of simple, polynomial shape functions [1].

In regard to the structure-borne noise, the most effective approach to reduce the noise is to modify components in the structural transfer path. Thus it is a common practice to develop large detailed computer models of the vehicle components using finite element (FE). Subsequently, the component models are integrated using substructuring techniques for analysis of the assembled system. The tire model is one such substructures, and the tire finite element model has been used since the 1970s. The number of elements was first considered to be only a few hundred. It is

currently a few million since the inclusion of the three-dimensional (3D) tread patterns and coupling between multiple subsystems/substructures [2,3]. The earliest models started with the 2D (two-dimensional) thin shell element models—axisymmetric and coarsely meshed tire models. These simplifications are adopted due to limited computational resources. The simulation output accuracy of the tire models is enough for the problem of interest. Now the models that inherit a 3D, full FEM, nonlinear fine mesh can capture the dynamic response of the tire with a high fidelity.

Typical FE numerical models for prediction of the tire/road noise consist of the wheel–tire–cavity structure model and tire/road contact model. These models can be divided into two categories: low-order analytical models and higher-order analytical models [4]. The low-order analytical models are based on analytical descriptions and physical insights, yielding computationally efficient numerical results that can be evaluated in a fast and efficient manner. However, correlating the parameters of these models to physical tire design parameters, such as reinforcement fiber angles, tire cross-section geometry, and rubber compound properties, is typically not possible. Furthermore, inherent nonlinear behavior of the tire due to, for example, rubber compounds and reinforcement materials, is typically not included in these models. Therefore the use of higher-order numerical tire models, where the models are built in a rigorous, mathematical way analogous to the real physical tire, appears to be more appropriate. These models include physical design parameters, such as rubber compounds and reinforcement fiber angles. They also allow different material properties to be described by dedicated constitutive models, using material test data rather than system-level tire measurement data. The detailed tire geometry can be replicated, given an adequate discretization of the tire cross-section and circumference. Hence, these high-fidelity models can be developed as a numerical predictive approach for tire design.

Many tire models are described based on nonlinear FE formulations. These FE formulations allow the inclusion of all sorts of nonlinearities, thereby enable the inclusion of a range of relevant physical effects such as nonlinear large strain behavior, incompressible material behavior, time and/or frequency-dependent viscous material behavior, and embedded reinforcement behavior.

Recently a fully nonlinear finite element model was combined with an arbitrary Lagrangian–Eulerian (ALE) formulation to describe both the rolling dynamics as well as the interaction between the tire and coarse

road surface [4]. In this model, a geometrical constraint approach is used to describe the tire/road interaction, rather than a constitutive approach, in order to keep the proposed method fully predictive and not relying on measurement data. However, the main shortcoming of a geometrical constraint approach is well known to be its large computational costs and simulation times. Therefore the nonlinear Multi-Expansion Modal Reduction/Hyperreduction method is applied to reduce the numerical computation costs and corresponding simulation times.

Despite the fast increase of computer performance over recent decades, it is still not possible to simulate the complete nonlinear dynamic behavior of rolling tires and subsequent sound radiation directly. A significant reduction of the computational cost can be achieved by employing a modal superposition technique. This leads to a computational strategy, where the tire/road noise is analyzed in several subsequent steps summarized as the following [5]:

- Computation of the nonlinear steady-state rolling analysis using the Modal Arbitrary Lagrangian–Eulerian (M-ALE) approach, which includes the effects of the rotation inertia and inflation pressure loads.
- Complex eigenvalue analysis for the steady state of the rolling tire.
- Determination of the excitation due to the texture of the road surface.
- Computation of the operational vibrations with modal superposition.
- Noise radiation analysis.

Due to the heterogeneity and nonlinear nature of the tires, the method of finite element analysis seems to be the only tool for reliable modeling of the behavior of such a system. A lot of commercial FE analysis software, such as ABAQUS, ANSYS, MSC, MARC, LS-DYNA, and HYPERWORKS are applicable.

### **10.2.1.2 Boundary element method**

The BEM, also known as the boundary integral equation method (BIEM), is an alternative deterministic method which incorporates a mesh that is only located on the boundaries of the domain and hence are attractive for free surface problems. There are two kinds of BEM. The direct one (DBEM) requires a closed boundary so that physical variables (pressure and normal velocity in acoustics) can only be considered on one side of the surface (interior or exterior), while the indirect one (IBEM) can consider both sides of the surface and does not need a closed surface. Both kinds of BEM are based on the direct solution of the Helmholtz equation.

The BEM has significant advantages over the FEM as there is no need for discretizing the domain under consideration into the elements, and this method only requires the boundary data as inputs. Therefore the meshing effort is limited, and the system matrices are smaller. However, the BEM also has disadvantages over the FEM; the BEM matrices are fully populated, with complex and frequency-dependent coefficients, which deteriorate the efficiency of the solution. Furthermore, singularities may arise in the solution, and these must be prevented [6].

BEMs can predict the sound radiation of a tire from the knowledge of the tire geometry and the surface velocity of the tire. BEMs can use the modal properties from the FE analysis. Therefore the tire geometry is readily identifiable, and the modal properties can be used to determine the velocity at any point on the surface of the tire. And the intensity of the sound radiation can be identified and tracked while design changes are made to the tire.

The BEM with nonreflecting boundary conditions and infinite elements is usually used to simulate the sound radiation based on the surface acceleration response of rolling tires [7]. Fig. 10.1 shows the 3D boundary element (BE) model with different filed point locations adapted from [7].

### 10.2.1.3 Waveguide finite element method

The WFEM is an FE-based approach by which approximate wave solutions are found for such structures or fluids. The method guides the waves in a single direction, such as the circumferential direction of the tire, with

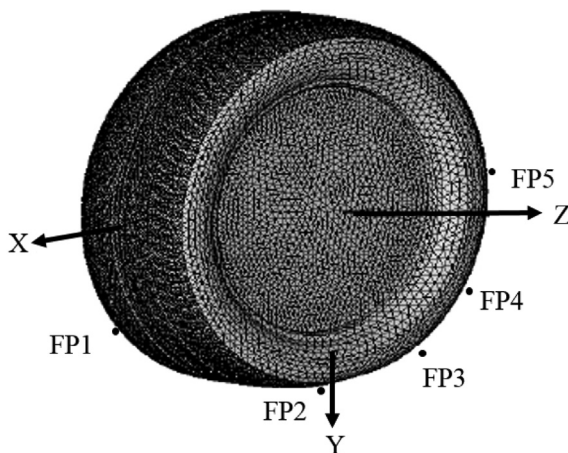


Figure 10.1 BE model with different point locations.

constant physical properties in that direction [8]. WFEM uses a 2D finite element model over the cross-section of the waveguide and describe the response of the tire in terms of a set of waves in that direction. The response of the nodes in direction  $X$  at time  $t$  is governed by the following equation:

$$\left[ \mathbf{K}_2 \frac{\partial^2}{\partial X^2} + \mathbf{K}_1 \frac{\partial}{\partial X} + \mathbf{K}_0 + \mathbf{M} \frac{\partial}{\partial t^2} \right] \mathbf{V}(X, t) = \mathbf{F}(X, t) \quad (10.1)$$

where  $\mathbf{K}_i$  is the stiffness matrix,  $\mathbf{M}$  is the mass matrix,  $\mathbf{F}(X, t)$  is a vector originating from the external load, and  $\mathbf{V}(X, t)$  contains all the nodal degrees of freedom (DOF).

The WFEM was used to investigate the vibrational behavior of tires. It uses special shell and solid waveguide finite elements to model the tire sidewalls, belt, and tread. The model has successfully been used to calculate the driving and transfer mobility, tire/road noise, and rolling resistance.

The main advantage of the WFEM as compared to standard FE formulations is the decreased calculation burden. This stems from the fact that only the cross-section is discretized, reducing the number of DOF introduced to the model. An additional advantage compared to conventional FE is that different wave-types are easy to identify and analyze, allowing for a somewhat deeper physical understanding of the investigated structure [9].

## 10.2.2 Energy methods at high frequency

In the high frequency range, when the dimension of the structure is considerably large with respect to the wavelength, conventional finite element analysis (FEA) requires a very large number of elements in order to properly capture the high frequency characteristics of a given structure. This consequently causes tremendously high computational costs and thus makes displacement-based FEA methods unfeasible [10]. On the other hand, SEA and ESEA can be used for simulating the vibroacoustic response of such large-scale structures at high frequencies within much less time.

### 10.2.2.1 Statistical energy analysis

SEA is an energy-based method for complex vibroacoustic problems at high frequencies. It is typically used for modeling the sound and vibration

energy dissipations and transmissions in the systems/subsystems such as vehicles, buildings, or industrial devices. It uses a combination of analytical, empirical, and experimental data. Since only local modes of SEA subsystems are required, the method is restricted to high frequency behavior.

A complex vibroacoustic system is modeled as an assembly of coupled subsystems. Coupling loss factors are defined as those that relate the energy flow to the subsystem energies. A power balance for each subsystem results in a set of linear algebraic equations that can be solved for the vibratory energy of each subsystem. Structural displacements and acoustic pressures are then computed from the energy results [11,12]. The application of SEA requires an accurate estimation of the parameters such as loss factors, as well as the modal density used in power balance equations because prediction accuracy depends on the estimation accuracy of the parameters. The modal density for a 3D rectangular annular sound field enclosed by rigid walls is given by:

$$n(\omega) = \frac{\omega^2 V}{2\pi^2 c^2} + \frac{\omega A}{8\pi c^2} + \frac{L}{16\pi c} \quad (10.2)$$

where  $V$  and  $A$  are the volume and surface area of the rectangular annular sound field, respectively;  $L$  is the total length of the edges of rigid walls.

From Langley [13] the model density for cylindrical shell is given by:

$$n_{II} = \left( \frac{k_0^2 S \Omega_R}{2\pi^2 \omega_R} \right) \int_{\theta_0}^{\theta_1} \sqrt{\frac{1}{\Omega_R^2 - \cos^4 \theta}} d\theta \quad (10.3)$$

$$n_I = \left( \frac{k_0^2 S \Omega_R}{2\pi^2 \omega_R} \right) \int_{\theta_1}^{\pi/2} \sqrt{\frac{1}{\Omega_R^2 - \cos^4 \theta}} d\theta \quad (10.4)$$

where  $n_{II}$  is the modal density of type 2 while  $n_I$  is of type 1. Type 2 refers to waves and modes with a lower value of  $k_2$  characterized by waves with motion restricted by in-plane stiffness, while type 1 corresponds to waves and modes with a large value of  $k_1$  characterized by waves with motion restricted by flexural stiffness of the cylinder wall.

In the SEA model of the tire-cavity, the acoustic radiation loss factor becomes related to the coupling loss factor when the annular acoustic cavity couples with the cylindrical shell. Therefore the coupling loss factor from the cylindrical shell to the annular cavity  $\eta_{12}$  is given by [14]:

$$\eta_{12} = \frac{2\rho_0 c \sigma}{\omega \rho_{sa}} \quad (10.5)$$

where  $\rho_0$  is the density of the cavity fluid,  $c$  is the speed of sound,  $\sigma$  is the radiation efficiency,  $\omega$  is the center frequency of a frequency band, and  $\rho_{sa}$  is the surface mass density.

The reciprocity relationship between the two subsystems is given by

$$n_1 \eta_{12} = n_2 \eta_{21} \quad (10.6)$$

The coupling loss factor from the annular cavity to the cylindrical shell is given by:

$$\eta_{21} = \frac{2\rho_0 c \sigma n_1}{\omega \rho_{sa} n_2} \quad (10.7)$$

where  $n_1$  is the cylindrical shell modal density and  $n_2$  is the annular cavity modal density.

It can be seen clearly from Eq. (10.7) that the tire–cavity coupling relationship depends on the accurate evaluation of the radiation efficiency. The radiation efficiency in the whole frequency bands containing some acoustically fast modes is given by [15] as:

$$\sigma \approx \frac{\Omega_R^{\frac{3}{2}} (f_R/f_c)}{4B} \sqrt{12(1-\nu^2)} \quad (10.8)$$

$$B = \frac{n(\omega)\pi h \omega_R}{L} \quad (10.9)$$

where  $f_R$  is the ring frequency while  $\nu$  is the Poisson's ratio,  $f_c$  is the critical frequency for the cylindrical shell,  $L$  is the cylinder axial width.

There are many advantages for using the SEA method, such as a decrease in computation time, but there are also a number of disadvantages. For example, SEA cannot produce a detailed response prediction, and only generates the spatial, frequency, and ensemble average values. It is therefore not possible to use SEA for detailed modal or natural resonant frequency analysis. Also, due to the high modal overlap requirement in SEA, accurate results are often limited to those in higher frequencies.

In recent years, variance models for SEA based on a perturbation approach have been implemented. The method has been validated experimentally to be able to provide an accurate prediction of the variance.

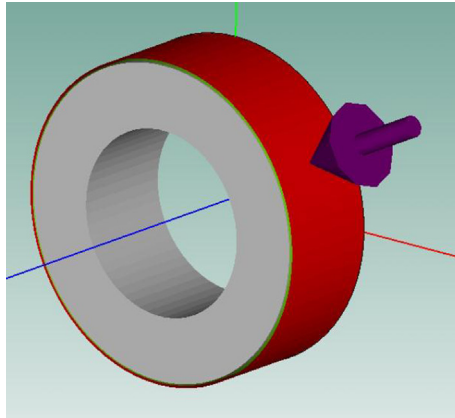


**Figure 10.2** SEA model of the tire–cavity.

While SEA generally predicts the mean energy level, which is an important indication of the expected response, the addition of the variance provides a more complete description of the statistical response of the system. A display model of the tire–cavity using AutoSEA [14] is shown in Fig. 10.2.

#### **10.2.2.2 Energy finite element analysis**

EFEA is a finite element–based computational method for high frequency vibration and acoustic analysis [16]. The EFEA applies finite element discretization to solve the governing differential energy equations. The primary variable in EFEA is defined as the time averaged energy density over a period and space averaged energy density over a wavelength.

The EFEA is compatible with low frequency FEM models since it can use an FEM database. This permits modeling flexibility and cost–saving as one FE model can be applied to both low and high frequency analysis. The prediction of a spatially varying energy level within a structural subsystem is available with the EFEA computation. The postprocessing of EFEA results also provides straight–forward visualization of the energy flow in a system, which is convenient for diagnoses and control of noise propagation.

EFEA can be applied to model highly damped or nonuniformly damped materials, and to model distributed masses as well as multipoint power input. Due to the utilization of the finite element technique, EFEA also has the other advantages that traditional FEM does not have.

It can be easily applied to irregular domains and geometries that are composed of different materials or mixed boundary conditions.

Although SEA models result in a few of equations which are easy to solve, they cannot be developed from CAD data, local damping cannot be accounted for, and the model development requires specialized knowledge. In contrast, EFEA offers an improved alternative formulation to the SEA for simulating the structural-acoustic behavior of built-up structures. It is based on deriving governing differential equations in terms of energy density variables and employing a finite element approach for solving them numerically. There are several advantages offered by EFEA. These advantages include the generation of the numerical model based on geometry; spatial variation of the damping properties can be considered within a particular structural member; the excitation can be applied at discrete locations on the model, and EFEA can be applied to the high frequency range, which benefits the large community of FEA users. These unique capabilities make the EFEA method a powerful simulation tool for design and analysis.

### 10.2.3 Hybrid methods in the mid frequency range

In between the low frequency application range of the deterministic methods and the high frequency application range of the SEA methods, there still exists the mid frequency range, for which currently mature prediction methods are required [17].

The prediction of the response of a vibroacoustic system in this mid frequency range faces two major difficulties due to a relatively short wavelength. Firstly, many DOF are required to capture the deformation details of the system, and secondly the response of the system can be sensitive to imperfections, so that manufacturing uncertainties can lead to significant variability in the performance of nominally identical items [17].

Recently, SEA is combined with deterministic method to simulate the characteristics of the tire-cavity coupling [18]. While the deterministic method focuses on the cavity pressure response and the complaint wall vibration velocity response at low frequency, SEA focuses on the response at high frequencies. The tire-cavity coupling system is modeled as an annular cylinder, where the side and inner walls are assumed to be rigid, while the tire surface structure is assumed to be flexible. The vibration energy of the tire surface structure  $E_1$  is statistically calculated as follows:

$$E_1 = \frac{\Pi_1 + \omega E_2 \frac{\eta_1(\omega)}{\eta_2(\omega)} \eta_{12}}{\omega(\eta_1 + \eta_{12})} \tag{10.10}$$

where  $\Pi_1$  is the power input to the tire structure,  $\omega$  is the angular frequency,  $\eta_1$  and  $\eta_2$  are the damping loss factors of the tire structure and the tire cavity,  $\eta_{12}$  is the coupling loss factor from the tire surface structure to the tire cavity.

The acoustic energy  $E_2$  of the tire cavity is given by:

$$\overline{E_2} = \frac{1}{V} \iiint_V \frac{1}{2} \int_{\omega_1}^{\omega_2} |p_\omega^2(r, \theta, z)|^2 \frac{\pi W (R_0 - R_i)^2}{\rho_o c^2} d\omega dV \tag{10.11}$$

where  $V$  is the volume of the cavity,  $\omega_1$  and  $\omega_2$  are the lower and upper limits of the frequency band,  $p_\omega$  is the root mean square time- and space-averaged pressure of the cavity obtained from experiment,  $r, \theta,$  and  $z$  are cylindrical coordinates,  $W$  is the tire width,  $R_0$  and  $R_i$  are the outer and inner radii of the tire cavity, respectively,  $\rho_o$  is the air density, and  $c$  is the speed of sound in air.

Fig. 10.3 shows the cavity energy curve calculated from the analytical SEA method agreed well with those predicted with AutoSEA and measured experimentally [14].

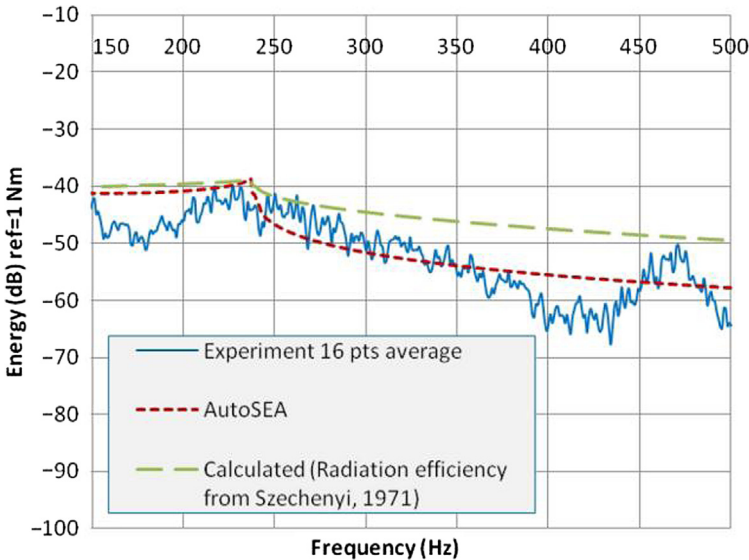


Figure 10.3 Mean cavity energy from the measurement, calculated, and AutoSEA simulation.

## 10.3 Other computer-aided engineering simulation methodologies

### 10.3.1 Computational fluid dynamics

CFD is a simulation tool that combines a numerical solution and analytical or mathematics solution to model fluid flow situations. CFD tries to determine the numerical solution of the equations that rule the fluids' flow, while the analytical or mathematic solution obtains the complete numerical description of the flow field studied in space and time.

The CFD of the tire model employs a large eddy simulation (LES) turbulence modeling approach which requires the Navier–Stokes (N–S) equations to be solved for simple groove geometries with a moving bottom wall that represents the deformation during the tire movement along the road surface. The alternative modeling approach uses the lattice Boltzmann method (LBM) which is a special discretization of the continuum Boltzmann equation in space, time, and velocity and uses the very large eddy simulation (VLES) approach for turbulence modeling.

Successful CFD analysis requires the boundary conditions to be defined at the boundaries of the flow domain which enable all the boundary variables to be calculated. It also requires the initial conditions of the solution variables for steady state or transient simulation to be defined.

Recently, CFD and the FEM were successfully combined to study the hydroplaning effect on the tire. These studies suggested that a car should travel on wet roads with low to mid speeds less than 65–85 km/h in order to avoid aquaplaning.

### 10.3.2 Transfer path analysis

TPA is a simulation tool used to identify structure-borne and airborne energy transfer routes from the excitation source to a given receiver location in the low-mid frequency range. In principle, TPA is applied to evaluate the contribution along each transfer path from the source to the receiver, so that one can identify the components along that path that need to be modified to solve a specific problem, and perhaps to optimize the design by choosing desirable characteristics for these components.

TPA can be applied to solve many vibroacoustic issues in manufacturing industries. Performing TPA on a car engine mounting system helps reduce interior noise, on driving wheel suspension and seating systems helps reduce the system vibration, and thus improve the driver and passenger comfort. Road noise disturbance in a vehicle can be minimized

using the multi reference TPA technique. Nowadays, TPA is even employed to complement pass-by noise engineering methods so as to reduce the overall vehicle's pass-by noise. TPA can be combined with hybrid FE/experimental modeling for acoustic optimization of a design. Operational transfer path analysis (OPTA) can be used to analyze the tire/road noise at a certain receiver location, where an artificial head records the interior noise during this coast-down testing.

An entirely different analysis concept is used for TPA. For TPA a vehicle is characterized by its "noise paths" rather than by actual geometry.

The principal aim of TPA is to sum up all individual noise paths (individual noise sources multiplied by respective noise transfer function (NTF) or sensitivity) to the full vehicle noise or vibration response. Individual noise sources are typically mount forces, intake and exhaust orifice noise, powertrain noise radiation, high frequency noise, and underhood sound due to powertrain rigid body motion, etc. For the example of a powertrain mount, the respective noise source would be mount displacement multiplied by mount stiffness; the respective noise sensitivity would be  $p/F$  (sound pressure ( $p$ ) per unit excitation force ( $F$ )) or NTF.

The mathematical requirement for TPA methods itself is significantly lower than for FE or BE methods, but valid TPA models require representative data such as noise sensitivities, for example. If the latter cannot be predicted with high confidence, these TPA methods need to be based on the measured noise sensitivities. Hence these TPA methods will be "exact" only for installations of "new" powertrains into given structures. Noise sources can be determined from measurements or CAE analyses.

## 10.4 Vehicle suspension corner module simulation

The suspension system is the key component that transmits the forces generated at the tire contact patch to the vehicle body. The most important forces are those from the ground that react and balance the weight of the vehicle. These reactions are primarily taken up by the deflections of the suspension springs. However, modern suspensions are highly complex mechanisms comprising various links and joints. These links balance a significant proportion of the total tire forces particularly during cornering and braking, where significant shear stresses are generated at the contact patch.

The mathematical model of the vehicle which is capable of simulating the ride and handling characteristics of the vehicle has been developed and implemented in ADAMS/Car. MSC ADAMS is a mechanical system dynamics simulation tool widely used by chassis/suspension designers in automotive industry. It is a virtual prototype software which includes various interfaces for modeling, equation solving, optimization, simulation, and visualizing aids. It also enables users to import rigid body models from different CAD software and flexible bodies from packages like MSC Nastran [19]. The dynamic characterization modeling is characterized by various elements in the actual vehicle, such as coil springs, telescopic shock absorbers, and pneumatic wheels.

Fig. 10.4 shows the front suspension system modeled as double fishbone per wheel suspension mechanism, also called as the deformable parallelogram arrangement, with elastic elements (coil springs) and dissipative elements (telescopic hydraulic dampers) driven by a bi-articulated rod [19].

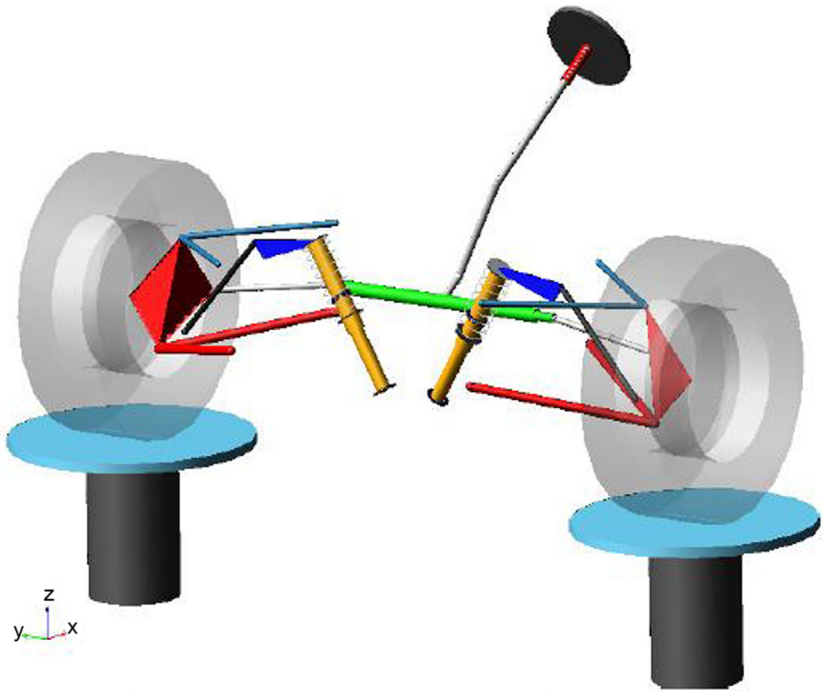


Figure 10.4 Front suspension system modeled in ADAMS-Car.

Although suspension and chassis systems are responsible for ride and handling characteristics of the vehicle, the tire is ultimately responsible for generating the control forces required to operate the vehicle. All these forces acting on the vehicle are either generated by the tire/road interface or by the aerodynamics effects, where at low speeds the aerodynamics effects can be ignored. Therefore the accuracy of the tire model describing the forces on the tire—road interface is thus of exceptional importance. It should ensure that the simulation model accurately represents the status of an actual vehicle.

For the simulation of pneumatic tires, the behavior of the tires has been characterized by different tire models which are incorporated in ADAMS/Tire such as PAC2002 Tyre Model, PAC-TMIE Tyre Model, Pacejka '89 Models', Pacejka '94 Models', and Fiala Model. The Pacejka models also known as the magic formulae is widely used to describe the tire forces in longitudinal and lateral directions [20]. The normal force of the tire is calculated for a tire deflection as:

$$F_z = \left\{ 1 = q_{v2}|\omega| \frac{R_0}{V_0} - \left( q_{F_{cx1}} \frac{F_x}{F_{z0}} \right)^2 - \left( q_{F_{cy1}} \frac{F_y}{F_{z0}} \right)^2 + q_{F_{c\gamma1}} \gamma^2 \right\} \left[ q_{F_{z1}} \frac{\rho}{R_0} + q_{F_{z2}} \left( \frac{\rho}{R_0} \right)^2 \right] F_{z0} + C_z \dot{\rho} \quad (10.12)$$

where  $F_z$  is the normal force,  $\omega$  is the rotational speed,  $\gamma$  is the camber angle, and  $q_{v2}$  is the tire stiffness verification coefficient with speed,  $q_{F_{cx1}}$  is the tire stiffness interaction with  $F_x$ ,  $q_{F_{cy1}}$  is the tire stiffness interaction with  $F_y$ ,  $q_{F_{c\gamma1}}$  is the tire stiffness interaction with camber,  $q_{F_{z1}}$  is the tire vertical stiffness coefficient (linear),  $q_{F_{z2}}$  is the tire vertical stiffness coefficient (quadratic),  $R_0$  is unloaded tire radius,  $\dot{\rho}$  is the tire deflection velocity, and  $C_z$  is the vertical tire damping coefficient.

When a vehicle undertakes a cornering operation, lateral force is developed at the tire—road contact area. This lateral force is dynamic force due to lateral acceleration of the vehicle and called a cornering force. It highly depends on the tire vertical load. As the vertical load of the tire increases under the cornering condition, the cornering force also increases. In addition, the cornering force also depends on the slip angle of the tire. As the slip angle increases under the same vertical load on the tire, the cornering force also increases.

## 10.5 Mechanisms of the wheel imbalance induced vibration

Tire/wheel imbalance results from the nonsymmetrical distribution of mass in a tire, wheel or other rotating component of the suspension system. Imbalance can be classified either static (in-plane imbalance) or dynamic (out-plane imbalance).

Static imbalance is confined to the wheel plane of the tire. It generates a periodic force variation at the axle in the vertical and longitudinal directions of a driven vehicle. Other sources of tire imbalance are large slips, multiple splices near the same circumferential location around the tire or mass rotation in other rotational components. A nonsymmetrical axis of rotation can also cause a static imbalance. The magnitude of the imbalance force is given by the following equation:

$$F = mr\omega^2 \quad (10.13)$$

where  $F$  is the imbalance force,  $m$  is the imbalance mass,  $r$  is the effective radius, and  $\omega$  is the rotational speed.

While dynamic imbalance results from nonsymmetric mass distribution along the axis of rotation, this produces an overturning moment variation about the longitudinal axis and aligning moment variation about the vertical axis. It can cause a vibration of the vehicle steering system.

## 10.6 Tire–road interaction caused by dynamic force variation induced by a hexagon tire

Tire force variation or nonuniformities is caused by material or manufacturing irregularities that can generate varying forces and moments at the axle of the tire/wheel assembly. These nonuniformities forces and moments are usually measured in either low-speed balancing machines for factory/shop or high-speed balancing machines for research. These forces and moments are periodic and if the rotational speed of the tire is known, then the frequency of any harmonic order at any test speed can be determined by the following equation:

$$f = N \times RPS \quad (10.14)$$

where  $f$  is the frequency,  $N$  is harmonic order, and  $RPS$  is the number of revolutions per second of the rotating tire.

As the speed of the tire increases, the frequencies of the harmonic orders will also increase. At some point the frequency of a harmonic will

coincide with a resonant frequency of the tire, and the level of the vibration amplitude will increase dramatically. Any force and moment variation can potentially cause a ride disturbance, but the experience has shown the vibrations in the radial (vertical) and longitudinal (fore/aft or drag) directions are the most important contributors of the ride disturbance. In addition, the dynamic imbalance induced aligning moment resonance can cause a torsional vibrational disturbance of the steering wheel of the vehicle. The longitudinal force variation is proportional to the radial runout of the tire and the square of the velocity which is given by

$$F \propto V^2 \Delta R K \quad (10.15)$$

where  $V$  is the vehicle velocity,  $\Delta R$  is the radial runout, and  $K$  is constant.

## 10.7 Tire–road interface impact force and friction force-induced vibration

The friction between the tire and the pavement is a complex phenomenon depending on many factors such as viscoelastic properties of rubber, pavement texture, temperature, vehicle speed, slip ratio, and normal pressure of the contact patch. Experiments have shown that the friction between the tire and the pavement is dependent on the vehicle speed and on the slip ratio during the vehicle maneuvering processes, such as braking, accelerating, or cornering [21]. The analysis of tire–pavement contacts requires not only understanding the material properties of the tire; but also, the knowledge of the vehicle operation and pavement surface condition. It is expected that the development of tangential contact stress is related to the frictional behavior of the contact surfaces. The formulation of slipping/adhesion zones in the contact area would change depending on the allowed maximum friction force before tire slipping. However, obtaining an accurate description of the frictional relationship is difficult when modeling the tire–pavement interaction. Therefore an appropriate friction model is needed to accurately capture the realistic interaction between the tire and pavement at various tire rolling speeds.

The development of the friction force between the rubber and rough hard surface depends on two effects that are commonly described as the adhesion and hysteretic deformation, respectively. The adhesion component is the result of the interface shear and is significant for a clean and smooth surface. The magnitude of adhesion component is related to the

product of the actual contact area and the interface shear strength. The hysteresis component is the result of the rubber damping losses related to energy dissipation which is caused by surface asperities [22]. Hysteric friction is enhanced with a rise in temperature [23].

Pavement friction is defined as the retarding tangential force developed at the tire–pavement interface that resists longitudinal sliding when braking forces are applied to the vehicle tires or sideways sliding when a vehicle steer around a curve. The sliding friction coefficient is calculated by:

$$\mu = \frac{F_h}{F_v} \quad (10.16)$$

where  $\mu$  is the sliding friction coefficient,  $F$  is the tangential force at the tire–pavement surface, and  $F_v$  is the vertical load on tire.

There are a number of friction models which have been developed to characterize the tire–pavement friction behavior for vehicle dynamics and stability control. The magic formula is well-known empirical model used in vehicle handling simulations, and given by [24]:

$$F(s) = c_1 \sin(c_2 \arctan(c_3 s - c_4 (c_3 s - \arctan(c_3 s)))) \quad (10.17)$$

where  $F(s)$  is the friction force due to braking or lateral force or self-aligning torque due to cornering,  $c_1$ ,  $c_2$ ,  $c_3$  are model parameters, and  $s$  is the slip ratio or slip angle.

The slip angle is the angle between the actual rolling direction of the tire and the direction toward which it is pointing. The slip ratio is defined by:

$$s = \frac{V - \omega \cdot r}{V} \cdot 100\% = \frac{V_s}{V} \cdot 100\% \quad (10.18)$$

where  $s$  is the slip ratio,  $V$  is the vehicle travel speed,  $\omega$  is the angular velocity of the tire,  $r$  is the free rolling radius, and  $V_s$  is the slip speed. When the tire is free rolling there is no slip, so the slip speed and slip ratio are both zero. When the tire is locked, the slip speed is equal to the vehicle speed and the slip ratio is 100%.

## 10.8 Finite element modeling of tire–pavement interaction

The modeling of the tire–pavement interaction is generally simulated in three steps. First, the axisymmetric tire model was loaded with uniform tire inflation pressure at its inner surface. Second, the 3D tire model was

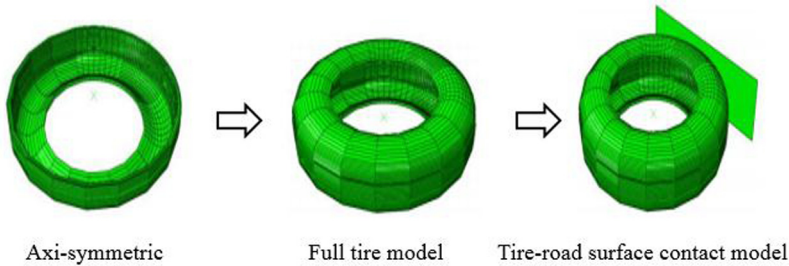


**Figure 10.5** Tire and road surface contact model in ABAQUS.

generated and placed in contact with the pavement under the applied load. In order to generate the 3D model of the tire, the symmetric model generation function is used in ABAQUS to transform the 2D model into 3D. As a result of this transformation, all axisymmetric elements CGAX4H and CGAX3H are converted into solid elements C3D8H and C3D6H respectively. Finally, the tire was rolled on pavement with different angular velocities and transport velocities. The tire rolling process is usually modeled using steady-state transport analysis in ABAQUS/Standard as shown in Fig. 10.5. The tire is designed as an axis-symmetric sketch then the sketch revolved around the axis and then it is mirrored about the symmetric plane. Finally, the tire road surface contact is created.

The hyperelasticity is initially modeled by Neo-Hookean and Mooney–Rivlin which is based on the rubber strain energy. The strain energy function with first and second strain invariants can be expressed as following [25]:

$$W = C_{10}(\bar{I}_1 - 3) + C_{01}(\bar{I}_2 - 3) \quad (10.19)$$

where  $C_{10}$  and  $C_{01}$  are the material constants experimentally determined,  $\bar{I}_1$  and  $\bar{I}_2$  are the first and second invariant of the unimodular component of the left Cauchy–Green deformation tensor and can be defined by [25]:

$$\bar{I}_1 = \bar{\lambda}_1^2 + \bar{\lambda}_2^2 + \bar{\lambda}_3^2 \quad (10.20)$$

$$\bar{I}_2 = \bar{\lambda}_1^{(-2)} + \bar{\lambda}_2^{(-2)} + \bar{\lambda}_3^{(-2)} \quad (10.21)$$

The  $\bar{\lambda}_1$  is the deviatoric stretch and is given by:

$$\bar{\lambda}_1 = J^{-1/3} \lambda_i \quad (10.22)$$

where  $J$  is the total volume ratio and  $\lambda_i$  is the principal stretch that is expressed as:

$$\lambda_i = 1 + \varepsilon_i \quad (10.23)$$

where  $\varepsilon_i$  is the principal strain. It should be noted that in these formulas for incompressible and isothermal materials,  $J = 1$ , and  $\lambda_1 \lambda_2 \lambda_3 = 1$ .

In ABAQUS, the hyperplastic elements with reduced integration and hourglassing control are chosen for avoiding shear locking and hourglassing in simulation.

The rubber reinforcement for carcass and belts are usually modeled using rebar elements which allows meshing the cord section independent of the host element. This independent meshing avoids unwanted meshing problems, such as small element between composite layers. In order to implement rebar layer, the following information should be known a priori: rebar thickness, spacing, orientation, location, and material properties.

The contact force between the tire and the pavement surface consists of two components: one normal to the pavement surface and one tangential to the pavement surface. Therefore the ground is considered an analytical rigid surface, and surface to surface contact interface is established between the tire tread and road in order to avoid tire tread mesh penetrate the ground. The zero-gap contact is achieved by modeling the contact problem using a Lagrange multiplier method. The coulomb friction law is used to describe the tangential interaction between two contacting surfaces. The contact status is determined by nonlinear equilibrium (solved through iterative procedures) and governed by the transmission of contact forces (normal and tangential) and the relative separation /sliding between two nodes on the surfaces in contact. There are three possible conditions for the nodes at the interface: stick, slip, and separation (Eqs. 10.24,–10.26).

$$\text{Stick condition : } g = 0; p < 0; \text{ and } [\tau_{11}^2 + \tau_2^2]^{0.5} < \mu \cdot p \quad (10.24)$$

$$\text{Slip condition : } g = 0; p < 0; \text{ and } [\tau_{11}^2 + \tau_2^2]^{0.5} = \mu \cdot p \quad (10.25)$$

$$\text{Separation condition: } g > 0; p = 0; \text{ and } \tau = 0 \quad (10.26)$$

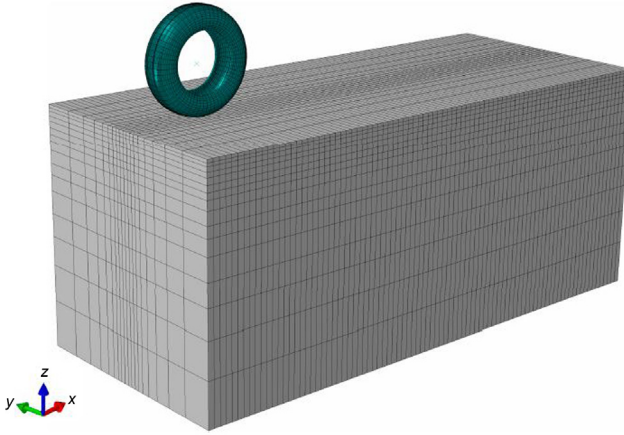


**Figure 10.6** 3D tire–pavement contact model.

where  $p$  is the normal force or pressure (compression is negative),  $g$  is the gap between two contact nodes,  $\tau_1$  and  $\tau_2$  are tangential forces or shear stress, and  $\mu$  is the friction coefficient.

By using the above methods, Fig. 10.6 shows 3D tire–pavement contact model for a groove tire (175SR14) [7].

## 10.9 Auralization models of tire/road noise

A powerful method in the product sound design process is to take advantage of the strengths of both recordings and simulations and combine them into auralization. Kleiner et al. [26] defined auralization as the process of rendering audible the sound field of a source in a space, by physical or mathematical modeling, in such a way as to simulate the binaural listening experience at a given position in the modeled space. According to Vorländer [27], auralization is the technique for creating audible sound files from numerical (simulation, measured, synthesized) data. Auralization can be seen as a hybrid model resulting in a time domain simulation. The required level of details in auralization depends on the stage in the development process. In an early development stage audible errors and artifacts may be acceptable as long as the main character of the sound is realistic.

Auralization of the structure-borne tire noise is created by combining each DOF of the hub forces and moments, with the impulse response of the corresponding DOF of the binaural transfer functions (BTFs). Then the operationally measured or simulated hub forces in six DOFs are

filtered through experimentally measured BTFs from the hub to an artificial head in the cabin of the car. To accurately simulate the hub forces and moments, a detailed and complex computer model of a wheel is needed. This requires that not only correct material properties of the compounds and layers of the tire, but also correct material properties of the rim are available. The boundary conditions of the rim/hub interface as well as the tire/road interaction including the texture of the road surface should also be included in the simulation. Due to the complexity, the tire models are simplified to various degrees. By changing the transfer functions or tire material properties, the model can be used to auralize and evaluate tire noise in an early design phase.

### **10.10 Trends and challenges in computer-aided engineering modeling of tire/road noise**

CAE is widely considered as an essential part of the noise and vibration refinement process in vehicle development. Therefore the current trends in CAE modeling of the tire/road noise are summarized as:

- A significant tire/road noise is expected to be audible as the power-train noise of modern vehicles tends to decrease or become less.
- Increasing efforts are currently being made by the tire and automotive industries to accurately model the tire/road noise.

The major challenges in the tire/road simulation are:

1. The greatest challenge is to develop a fast and accurate model for understanding and simulating the tire/road interaction problem.
2. Another challenge is to develop better material models for both rubber and reinforcing components.
3. Tire simulation models have to represent stationary forces and moments due to the tire deflection and longitudinal and lateral slips.
4. Tire asymmetries due to the conicity and plysteer effects have to be included in the tire simulation models.
5. Thermal effect aspects of the tire properties become very important to be understood as they are motivated by car racing applications involving extreme safety maneuvers.
6. Efficient modeling of the tread pattern is very important and influences many tire performances such as traction, wear, hydroplaning, noise, and vibration.
7. Tires are modeled by considering the nonisothermal conditions for the prediction of the temperature rise and energy losses in the tire.

8. Tire simulation models for the contact pavement materials of soil, snow, mud, and other soft materials, and noise generation models should be developed, especially in high frequency ranges.

## 10.11 Summary

There have been significant efforts made to increase the reliance on CAE technology in modeling tire/road interaction induced noise, accompanied by a trend to reduce or eliminate prototype testing time during the early design phase. These CAE models should integrate the parameters describing both the tire and the road surface. The interaction mechanisms between the tire and road surface are complex, which makes it difficult to be modeled through the extremely complicated mathematical expressions or equations. This chapter explains that there are models able to simulate the tire–pavement interaction induced noise either through all the mechanisms, or through just some of the mechanisms.

The chapter has discussed a very broad range of tire/road noise simulation models. These models were compared in terms of the frequency spectrum range, applications, parameters, etc. It can be reasonably assumed from the preceding discussion that the FEM is still the most suitable technique for examining the tire/road interaction induced noise. This is primarily due to the fact that FEM can model the complete tire structure and take into account almost all other relevant physical phenomena. In accompanying this, the BEM is successfully applied to model the sound radiation of the tire.

## Nomenclature

$\mathbf{K}_i$	the stiffness matrix
$\mathbf{M}$	the mass matrix
$\mathbf{F}(X, t)$	vector originating from the external load
$\mathbf{V}(X, t)$	vector contains all the nodal degrees of freedom
$n(\omega)$	the modal density of a 3D rectangular annular sound field enclosed by rigid wall
$V$	the volume of the rectangular annular sound field
$A$	the area of the rectangular annular sound field
$L$	the total length of the edges of rigid walls
$n_{II}$	the modal density of type 2
$n_I$	the modal density of type 1
$\sigma$	the radiation efficiency
$\rho_{sa}$	the surface mass density
$\eta_{12}$	the coupling loss factor from cylindrical shell to the annular cavity

$\eta_{21}$	the coupling loss factor from the annular cavity to the cylindrical shell
$f_R$	the ring frequency
$\nu$	the Poisson's ratio
$f_c$	the critical frequency of the cylindrical shell
$L$	the cylindrical axial width
$E_1$	the vibration energy of the tire structure
$\omega$	the angular frequency
$\eta_1$	damping loss factor of the tire
$\eta_2$	damping loss factor of the acoustic cavity
$\eta_{12}$	the coupling loss factor from the tire structure to the tire cavity
$\Pi_1$	the power input
$E_2$	the acoustic energy of the tire cavity
$V$	the volume of the cavity
$\omega_1$	the lower limits of the frequency
$\omega_2$	the upper limits of the frequency
$p_\omega$	the time- and space-averaged rms pressure of the cavity
$\rho_0$	the density of sound in air
$c$	the speed of sound in air
$W$	the tire width
$F_z$	the normal force
$\omega$	the rotational speed
$\gamma$	the camber angle
$q_{Fz1}$	the tire vertical stiffness coefficient (linear)
$q_{Fz2}$	the tire vertical stiffness coefficient (quadratic)
$q_{v2}$	the tire stiffness verification coefficient with speed
$q_{F\alpha 1}$	the tire stiffness interaction with $F_x$
$q_{F\gamma 1}$	the tire stiffness interaction with $F_y$
$q_{F\gamma 1}$	the tire stiffness interaction with camber
$R_0$	the unloaded tire radius
$\dot{\rho}$	the tire deflection velocity
$C_z$	the vertical tire damping coefficient
$F$	the imbalance force
$m$	the imbalance mass
$r$	the effective mass
$N$	the harmonic order
$RPS$	the revolutions per second of the tire
$\mu$	the sliding friction coefficient
$F_h$	the tangential force at the tire–pavement surface
$F_v$	the vertical load on tire
$F(s)$	the friction force due to braking or lateral force
$s$	the slip ratio or slip angle
$V$	the vehicle travel speed
$V_s$	the slip speed
$W$	the strain energy function
$\bar{I}_1$	the first invariant of the unimodular component of the left Cauchy–Green deformation tensor
$\bar{I}_2$	the second invariant of the unimodular component of the left Cauchy–Green deformation tensor

$C_{10}$	the material constant
$C_{01}$	the material constant
$J$	the total volume ratio
$\lambda_i$	the principal stretch
$\varepsilon_i$	the principal strain

## References

- [1] Donders S. Computer-aided engineering methodologies for robust automotive NVH design [Ph.D. thesis]. K.U. Leuven, Department of Mechanical Engineering, Division PMA, Leuven, Belgium; 2008. Available online: <<http://hdl.handle.net/1979/1698>>.
- [2] Surendranath H, Dunbar M. Parallel computing for tire simulations. *Tire Sci Technol* 2011;39(3):193–209.
- [3] Nakajima Y. Application of computational mechanics to tire design—yesterday, today, and tomorrow. *Tire Sci Technol* 2011;39(4):223–44.
- [4] De Gregoriis D, Naets F, Kindt P, Desmet W. Development and validation of a fully predictive high-fidelity simulation approach for predicting coarse road dynamic tire/road rolling contact forces. *J Sound Vib* 2019;452:147–68.
- [5] Brinkmeier M, Nackenhorst U, Petersen S, Von Estorff O. A finite element approach for the simulation of tire rolling noise. *J Sound Vib* 2008;309:20–39.
- [6] Katsikadelis JT. *Boundary elements theory and applications*. Amsterdam: Elsevier; 2002. XIV + 336, ISBN 978-0-080-44107-8.
- [7] Wang G, Zhou H. Boundary element analysis of rolling tire noise. In: International conference on transportation mechanical and electrical engineering (TMEE); 2011.
- [8] Li T, Burdisso R, Sandu C. Literature review of models on tire–pavement interaction noise. *J Sound Vib* 2018;420:357–455.
- [9] Fraggstedt M. Power dissipation in car tyres, licentiate thesis. Department of Aeronautical and Vehicle Engineering, Royal Institute of Technology; 2006. Available at: <[http://www.ave.kth.se/publications/mwl/downloads/TRITA-AVE\\_2006-26.pdf](http://www.ave.kth.se/publications/mwl/downloads/TRITA-AVE_2006-26.pdf)>.
- [10] Amoroso F, De Fenza A, Linari M, Di Giulio M, Lecce L. Energy finite element analysis (EFEA) approach for fuselage noise prediction. *Noise and vibration: emerging methods*. Sorrento; April 1–4, 2012.
- [11] Mace B. Statistical energy analysis, energy distribution models and system modes. *J Sound Vib* 2003;264(2):391409.
- [12] Langley R, Shorter P, Cotoni V. A hybrid FE-SEA method for the analysis of complex vibro-acoustic systems. In: Proceedings of the NOVEM 2005 conference, Saint-Raphael, France; 2005.
- [13] Langley R. The modal density and mode count of thin cylinders and curved panels. *J Sound Vib* 1994;169(1):43–53.
- [14] Mohamed Z, A study of tyre cavity resonance noise mechanism and countermeasures using vibroacoustic analysis [Ph.D. thesis]. School of Aerospace, Mechanical & Manufacturing Engineering, RMIT University, Australia; August 2014.
- [15] Szechenyi E. Modal densities and radiation efficiencies of unstiffened cylinders using statistical methods. *J Sound Vib* 1971;19:65–81.
- [16] Zhang W, Wang A, Vlahopoulos N, Wu K. High frequency vibration analysis of thin elastic plates under heavy fluid loading by an energy finite element formulation. *J Sound Vib* 2003;263:21–46.
- [17] Desmet W. Mid-frequency vibro-acoustic modelling: challenges and potential solutions. In: Proceedings of ISMA, Leuven, Belgium; 2002. p. 835–62.

- [18] Mohamed Z, Wang X. A deterministic and statistical energy analysis of tyre cavity resonance noise. *Mech Syst Signal Process* 2016;70–71:947–57.
- [19] Wideberg J, Bordons C, Luque P, Mantaras DA, Marcos D, Kanchwala H. Development and experimental validation of a dynamic model for electric vehicle within hub motors. *Proc Soc Behav Sci* 2014;160:84–91.
- [20] Pacejka HB. *Tire and vehicle dynamics*. Butterworth-Heinemann; 2002.
- [21] Henry JJ. Evaluation of pavement friction characteristics, NCHRP synthesis 291, TRB, National Research Council, Washington, DC; 2000.
- [22] Wang H, Al-Qadi IL, Stanciulescu I. Effect of friction on rolling tire–pavement interaction. In: USDOT Region V Regional University Transportation Center final report; 2010.
- [23] Yu M, Wu G, Kong L, Tang Y. Tire–pavement friction characteristics with elastic properties of asphalt pavements. *Appl Sci* 2017;7:1123.
- [24] Pacejka HB. *Tire and vehicle dynamics*. 2nd ed. Butterworth-Heinemann; 2006.
- [25] Yang X. Finite element analysis and experimental investigation of tyre chrematistics developing strain-based intelligent tyre system [Ph.D. thesis]. Mechanical engineering, University of Birmingham, Birmingham, UK, September 2011.
- [26] Kleiner M, Dalenbäck BI, Svensson P. Auralization—an overview. *J Audio Eng Soc* 1993;41(11):861–75.
- [27] Vorländer M. *Auralization; fundamentals of acoustics, modelling, simulation, algorithms and acoustic virtual reality*. RWTH edition Springer; 2008.